

# A Boundary Element-Finite Element Procedure For Porous and Fractured Media Flow

DEREK ELSWORTH

*Department of Mineral Engineering, Pennsylvania State University, University Park*

A coupled boundary element-finite element procedure is presented for linear and nonlinear fluid flow simulation in porous and fractured aquifers. Quadratic variation of both element geometry and fundamental singularity is used in the constitutively linear direct boundary element formulation. Compatible 3- to 9-noded Lagrangian finite elements are used to represent the plane flow domain for mixed linear and nonlinear flows, alike. Nodes on the external contour of the boundary element domain are only retained if flux boundary conditions are not prescribed, thus resulting in reduced matrix dimension. The geometric conductance of the linear boundary element region is evaluated only once. The resulting system matrices remain sparse, positive definite, and may be arranged for symmetry. Nonlinearity, in this context, is restricted to turbulent flow at high Reynolds numbers, although other nonlinearities may be easily accommodated using a similar procedure. A Missbach relationship is implemented to represent turbulent flow in rock fractures. Turbulent effects are confined to the finite element domain, and the resulting nonlinear equations are solved by direct iteration. Validation studies are completed against analytical solutions to linear and nonlinear flow problems. Excellent agreement is obtained with relatively sparing nodal coverage.

## INTRODUCTION

Numerical models provide an effective means of rapidly evaluating a number of comparative scenarios in the quantification of groundwater flows. The heterogeneous and discontinuous nature of rock aquifers, combined with the limited access and penetration of standard site investigation procedures, makes the acquisition and interpretation of basic hydrologic data extremely difficult. High-quality numerical simulation techniques therefore provide an extremely important tool with which the impact of varied engineering or resource exploitation schemes may be readily evaluated. Sensitivity analyses of this nature provide a firm basis upon which subsequent judgemental decisions may be made [Bachmat *et al.*, 1980].

Of the powerful numerical techniques available, formulations may be divided between domain and boundary formulations. Associated with individual models are intrinsic merits and demerits which regulate their performance in any set engineering situation. Domain formulations encompass finite element and finite difference methods and require that the interior of the flow field is suitably discretized. Conversely, boundary solution procedures require only that the external edge contours of separate hydraulic zones be delimited as in the direct and indirect boundary element methods.

Domain methods offer powerful attributes in that complex nonlinear flow behavior, such as that evident in partially saturated [Neuman, 1973] or turbulent flow [Elsworth, 1985], may be easily accommodated. The system matrices are nonfully populated and in many instances are sparse, allowing considerable economy in storage requirements and execution time. Further computational savings may be realized with the finite element class of domain solutions where elemental and global system matrices are guaranteed symmetric and positive definite for linear and nonlinear potential flow problems alike. The extensive meshing within the domain, however, exacerbates data input requirements and introduces additional inter-

nal degrees of freedom for which results are sometimes not required. Thus although the matrix bandwidth may be small, the number of active equations comprising the system may be extremely large.

Boundary solution procedures are ideally suited to problem geometries of large volume to surface area ratio (equidimensional). Relatively trivial meshing is required, the discretization being limited to the edge contour of hydraulically homogeneous zones. System matrices are, however, asymmetric and fully populated within identified hydraulic subregions. Additionally, the virtue exalted in requiring discretization over the domain contour only is negated if nonlinear analysis of the interior is attempted. Primarily for this reason, boundary solution methods have not enjoyed popular application to nonlinear problems.

Coupled boundary element-finite element procedures offer the potential of using each of the different numerical procedures in the environment to which they are best suited. The innate strength of domain methods in dealing with constitutive nonlinearity, together with the relatively favorable structure of the system matrices make them ideal candidates to describe the behavior of nonlinear regions embedded within otherwise linear systems. The effectiveness with which boundary element procedures may accommodate volumetrically large but constitutively linear domains presents an ideal medium with which the far field may be adequately represented. Nonlinear effects discussed in the following sections are restricted to turbulent flows in fractured and porous-fractured media.

## PREVIOUS APPLICATION

Previous applications of physical coupling between domain and integral methods are evident within the continuum mechanics literature. These applications span the fields of wave mechanics [Chen and Mei, 1974; Shaw, 1978], electrostatics [Silvester and Hsieh, 1971], and elastostatics [Brady and Wassnyg, 1981], although this list is not exhaustive. A fine summary and critical commentary on many of these methods is given in the work by Zienkiewicz *et al.* [1977]. Application to problems of Darcy fluid flow have been investigated by

TABLE 1. Equivalent Fracture Hydraulic Conductivities

Hydraulic Zone	Equivalent Hydraulic Conductivity $K_e$	Exponent $\alpha$
1	$\frac{gb^2}{12\nu}$	1.0
2	$\frac{1}{b} \left[ \frac{g}{0.079} \left( \frac{2}{\nu} \right)^{1/4} b^3 \right]^{4/7}$	4/7
3	$4g^{1/2} \log \left[ \frac{3.7}{k/2b} \right] b^{1/2}$	1/2
4	$\frac{gb^2}{12\nu(1 + 8.8(k/2b)^{3/2})}$	1.0
5	$4g^{1/2} \log \left[ \frac{1.9}{(k/2b)} \right] b^{1/2}$	1/2

Shapiro and Andersson [1983]. A coupled procedure to accommodate line finite elements representing fractures in two dimensional space was presented using constant singularity boundary elements and linear variation finite elements.

The following presents a coupled procedure using Lagrangian quadratic basis functions to represent element geometry and dependent variables at the interface between finite element and boundary element regions. Interelement compatibility is therefore strictly enforced. A method of straightforward coupling is used to condense out unnecessary nodal equations and application is investigated to linear and nonlinear flow problems.

#### FLOW NONLINEARITY

A generalized constitutive relationship for flow in saturated porous and fractured media may be represented by Darcy's law

$$v = -K \left( \frac{\partial \phi}{\partial x} \right) \frac{\partial \phi}{\partial x} \quad (1)$$

where  $v$  is the Darcy flow velocity,  $\partial \phi / \partial x$  is the driving hydraulic gradient, and  $K(\partial \phi / \partial x)$  is the gradient dependent hydraulic conductivity. The nonlinearity arises from mixed inertial and turbulent effects which operate simultaneously as flow velocities become significant. Both inertial and turbulent effects are manifest as increased flow impedance when Darcy velocities are increased. Inertial impedance results from spatial accelerations within the flow field that may commonly be attributed to converging flow. These effects have been observed experimentally and may be deduced based on consideration of momentum balance within the Navier-Stokes equations [Irma, 1958]. Turbulent effects may be evident at the high-flow velocities possible within open voided or fractured rock masses. Fractures, especially, provide open conduits in which high velocity flows may be realized under relatively modest hydraulic gradients. For rock fractures, the transition to turbulent flow is most conveniently indexed by recourse to the Reynolds number  $Re$  such that

$$Re = 2bv/\nu \quad (2)$$

where  $b$  is the nominal fracture aperture, and  $\nu$  is the fluid kinematic viscosity. The nondimensional Reynolds number is extremely useful in fracture flow applications in that it is possible to define the range over which certain hydraulic param-

eters are applicable. These hydraulic parameters are the constants in the commonly used Missbach and Forchheimer flow laws.

The Forchheimer law uses a polynomial expression to relate the Darcy velocity  $v$  to driving hydraulic gradient  $\partial \phi / \partial x$  as

$$\partial \phi / \partial x = \bar{a}v + \bar{b}v^2 \quad (3)$$

where  $\bar{a}$  and  $\bar{b}$  are experimentally determined parameters assumed constant over a given range of Reynolds numbers. The general correctness of this expression may be deduced from manipulation of the Navier-Stokes equations [Irma, 1958] with the constants  $\bar{a}$  and  $\bar{b}$  being properties of both the fluid and transmitting medium. For low velocity flows,  $\bar{a}$  is equivalent to the reciprocal of hydraulic conductivity and  $\bar{b}$  is near zero.

Despite the analytical robustness of the Forchheimer relationship, the more compact Missbach law has found greater favor within groundwater applications related to fracture hydrology [Louis, 1969] and flow in open voided materials [Leps, 1973] with some exceptions [Volker, 1969; 1975]. The Missbach law links Darcy velocity  $v$  to driving hydraulic gradient through a power relationship of the form

$$\partial \phi / \partial x = cv^e \quad (4)$$

where the proportionality constant  $c$  and the power exponent  $e$  are constant over given ranges of Reynolds number. The Missbach relationship of (4) may be inverted to yield

$$v = -K_e \left[ \frac{\partial \phi}{\partial x} \right]^{1/e} \quad (5)$$

where  $\alpha = 1/e$  and the equivalent hydraulic conductivity  $K_e$  is constant only over a given range of Reynolds numbers. For laminar flow,  $K_e$  is equivalent to the saturated hydraulic conductivity, and  $\alpha$  is unity. For fully turbulent flow in a rough-walled fracture, the equivalent hydraulic conductivity  $K_e$  may be determined empirically, and  $\alpha$  is equal to 1/2. Transition from laminar to turbulent flow is indexed by a critical Reynolds number  $Re_c$ . For rough-walled fractures, both the critical Reynolds number and the equivalent hydraulic conductivity are controlled by the ratio of mean fracture wall roughness to fracture double aperture  $k/2b$ . Experimentally derived suites of results are available [Louis, 1969] to quantify these parameters. Equivalent hydraulic conductivity magnitudes are given in Table 1 referring to the hydraulic zones, one through five, depicted in Figure 1. These results are germane to the following.

#### FINITE ELEMENT IMPLEMENTATION

The nonlinear hydraulic conductivity of (5) may be rearranged into a form directly analogous to Darcy's law for one dimensional flow as

$$v = - \left[ K_e \left[ \frac{\partial \phi}{\partial x} \right]^{\alpha-1} \right] \frac{\partial \phi}{\partial x} = -\bar{K} \frac{\partial \phi}{\partial x} \quad (6)$$

where  $\bar{K}$  is an equivalent scalar value of nonlinear hydraulic conductivity, and  $\alpha$  is set equal to 1 or 1/2 for laminar or turbulent flow, respectively. For two dimensional flow, the appropriate hydraulic conductivity tensor relating cartesian Darcy velocities to cartesian gradients is given by  $-\bar{K}I$  where  $I$  is the identity matrix. For multinoded plane elements, parametric representation of geometry ( $x, y$ ) and total hydraulic

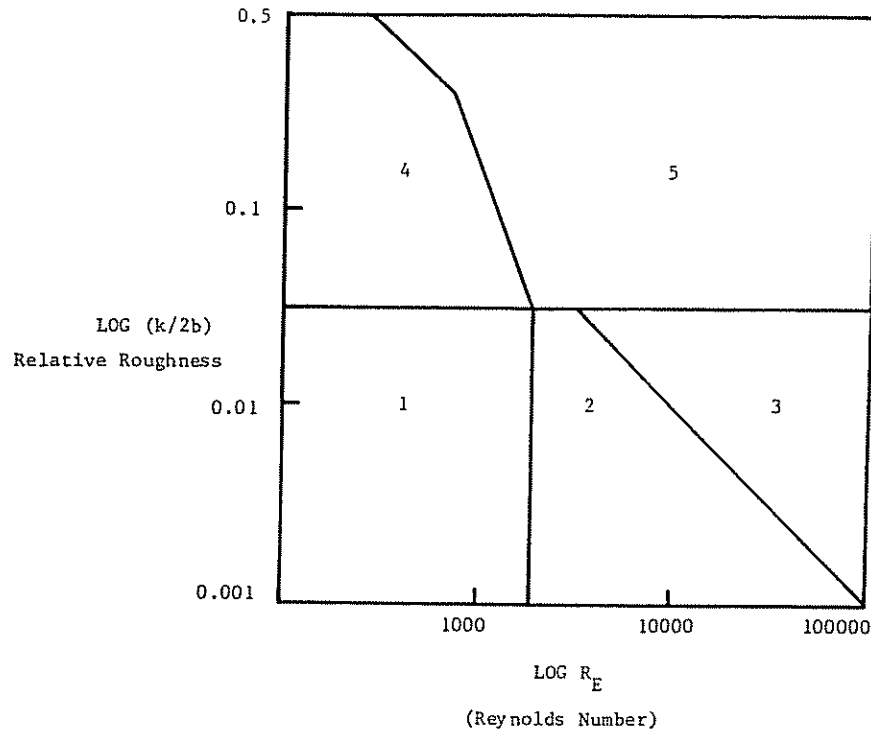


Fig. 1. Hydraulic zones for fracture flow [Louis, 1969].

head  $\phi$  is appropriate. The point values of any of these parameters within the bounds of a single element is therefore

$$x = \mathbf{h}^T \mathbf{x} \tag{7a}$$

$$y = \mathbf{h}^T \mathbf{y} \tag{7b}$$

$$\phi = \mathbf{h}^T \phi \tag{7c}$$

where  $\mathbf{h}^T$  is a vector of basis functions, the vectoral (boldfaced) quantities are nodal values, and the left-hand sides represent interpolated values. Since equivalent nonlinear hydraulic conductivity  $\bar{K}$  in the turbulent regime is a dependent function of hydraulic gradient,  $\bar{K}$  will, in general, vary within individual elements. Substituting Darcy's law of the form given in (6) into the normal Galerkin method and subsequently applying Green's theorem yields the matrix equation

$$\mathbf{q} = \mathbf{K}\phi \tag{8}$$

where  $\mathbf{q}$  is a vector of prescribed nodal discharges defined per unit area, and  $\mathbf{K}$  is a geometric conductance matrix. Equation (8) is equally valid at the elemental and global scales. For two dimensional analysis, the area integration required to evaluate the geometric conductance matrix  $\mathbf{K}$  at the elemental level is given by

$$\mathbf{K} = b \int_{\Omega} \mathbf{a}^T \bar{\mathbf{K}} \mathbf{a} \, d\Omega \tag{9}$$

where  $\mathbf{a}$  is a vector containing the derivatives of the shape functions  $\mathbf{h}$  with respect to global coordinates;  $\bar{\mathbf{K}}$  is a  $2 \times 2$  diagonal matrix (i.e.,  $-\bar{K}\mathbf{I}$ ) containing the magnitude of the equivalent nonlinear hydraulic conductivity  $\bar{K}$  at all nonzero entries; and  $\Omega$  is the area of the element. For the two-dimensional case, the thickness  $b$  is considered constant over a

single element and Lagrangian basis functions  $\mathbf{h}$  for a variable 3- to 9-noded element are used.

Rather than describe the variation of equivalent nonlinear hydraulic conductivity over the elemental domain using the nodal based shape functions of (7), the magnitude of  $\bar{K}$  may be readily evaluated at the internal Gauss points. Dual or triple point quadrature may be used to evaluate all integrals of (9) with a dual-point scheme having proved sufficiently accurate for all examples completed to date. Since, for the turbulent case,  $\bar{K}$  is a function of the maximum in-fissure hydraulic gradient, the magnitude of the gradients with respect to global coordinates are given as

$$\left\{ \begin{array}{l} \frac{\partial \phi}{\partial x} \\ \frac{\partial \phi}{\partial y} \end{array} \right\} = \mathbf{a}\phi \tag{10}$$

and the maximum hydraulic gradient is computed as the vector sum of the orthogonal components. Since the formulation is nonlinear with respect to nodal values of total head an iterative solution is implemented. For the global system, a laminar solution is first sought to provide initial nodal heads. This solution is used to evaluate hydraulic gradients and hence revise hydraulic conductivities. The direct iteration sequence employed is

$$\mathbf{K}^l = f(\mathbf{a}\phi^l) \tag{11}$$

$$q^{l+1} = \mathbf{K}^l \phi^{l+1} \tag{12}$$

where the superscripted  $l$  refers to the iteration cycle and  $f(\ )$  refers to "a function of." Only those elements in which the

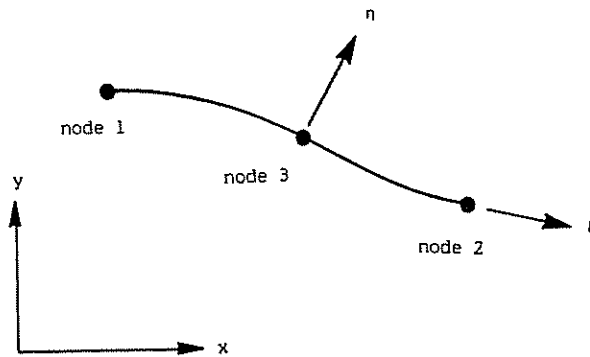


Fig. 2. Representation of a three-node isoparametric boundary element.

hydraulic conductivity  $K$  changes over a single-iteration cycle require to be reevaluated.

#### BOUNDARY ELEMENT ANALYSIS

To ensure effective coupling between the finite element and boundary element domains it is important that nonlinear effects propagating throughout the finite element region do not encroach into the boundary solution region. Under this proviso, the boundary domain is assumed to be constitutively linear and the formulation is able to operate in its most advantageous mode. In order that flow continuity between the domain and integral regions is maintained, the boundary element procedure must use basis functions compatible with those of the finite element region. For the boundary element procedure discussed in the following, isoparametric representation of both singularity and geometry is used. The element geometry is illustrated in Figure 2.

The boundary constraint equation corresponding to the direct formulation of the boundary element method may be stated as [Jaswon and Symm, 1977]

$$c(i)\phi(i) + \int_{\Gamma} V(i, j)\phi(j) d\Gamma = \int_{\Gamma} \Phi(i, j)v(j) \cdot n d\Gamma \quad (13)$$

where  $V(i, j)$  and  $\Phi(i, j)$  are kernel functions describing the influence effected at point  $j$  due to a unit source located at point  $i$ . The total hydraulic potential  $\phi(j)$  and normal to the boundary velocity  $v(j) \cdot n$  may be evaluated at any point on the boundary  $\Gamma$  from the kernel solutions. The free term  $c(i)$  is a function of the domain geometry and is equal to  $\delta_{ij}$  for an internal source and  $\frac{1}{2}\delta_{ij}$  where point  $i$  is located on a smooth boundary with  $\delta_{ij}$  being the Kronecker delta. For two dimensional porous media flow, the kernels for a line source are [Kellogg, 1953]

$$\Phi(i, j) = \frac{M}{2\pi} \ln r \quad (14a)$$

$$V(i, j) = \frac{-KM}{2\pi r} \quad (14b)$$

where  $r$  is radius ( $i$  to  $j$ );  $K$  is the formation hydraulic conductivity; and  $M$  is the source strength. Lagrangian basis functions are used to define the geometry of an element where (13) may be rewritten in terms of local coordinates for a single biunit line element as

$$c(i)\phi(i) + \int_{-1}^{+1} V(i, j)\phi(j) \frac{d\Gamma}{d\xi} d\xi = \int_{-1}^{+1} \Phi(i, j)v(j)n \frac{d\Gamma}{d\xi} d\xi \quad (15)$$

and the Jacobian is identified as

$$\frac{d\Gamma}{d\xi} = \left[ \left( \frac{dx}{d\xi} \right)^2 + \left( \frac{dy}{d\xi} \right)^2 \right]^{1/2} \quad (16)$$

with

$$x = \mathbf{h}^T \mathbf{x} \quad (17a)$$

$$y = \mathbf{h}^T \mathbf{y} \quad (17b)$$

$$\phi = \mathbf{h}^T \Phi \quad (17c)$$

$$v \cdot n = \mathbf{h}^T (v \cdot \mathbf{n}) \quad (17d)$$

where  $\mathbf{h}^T$  contains a different family of basis functions from those identified in (7) previous. The Lagrangian basis functions are one dimensional in this case, varying only over the length of the element and are represented in local coordinates as

$$\mathbf{h}^T = \frac{1}{2} [(1-\xi) - (1-\xi^2); (1+\xi) - (1-\xi^2); 2(1-\xi^2)] \quad (18)$$

where  $\xi$  represents the natural coordinates of the biunit element with  $-1 < \xi < 1$ . Similar functional variation for both heads and boundary velocities are used, each being of quadratic form. Since velocities are related to the gradient of head, it may be desirable to use interpolation one degree lower for velocities than that for heads. The results of validation studies completed did not warrant implementation of this constraint. Under parametric representation, the integrals of (15) are evaluated by Gauss quadrature for all nodes comprising the boundary element system [Stroud and Secrest, 1966; Elsworth, 1986b]. Where a sharp corner is encountered at a node, the  $V$  kernel integrations are completed on adjacent segments where there is slope continuity on each element segment. These quantities are then summed to yield the nodal weighted flux out of the region rather than represent flux in any particular normal (to the boundary) direction. For a system of  $m$  nodes, each with a single degree of freedom,  $m$  simultaneous equations result. In matrix format these may be represented as

$$\mathbf{V}\phi = \Phi v \cdot n \quad (19)$$

which, for  $m$  known or prescribed nodal boundary conditions yields a solvable set. After performing appropriate column interchanges on (19) to rearrange all known boundary conditions to the right-hand side vector, the identity may be solved to yield a geometric conductance matrix such that

$$[\Phi^{-1}\mathbf{V}]\phi = v \cdot n \quad (20)$$

which is of similar form to the finite element statement of (8). Premultiplying (20) by the ranked cross-sectional area of flow will convert Darcy flow velocities directly to discharge quantities such that

$$\mathbf{q} = b \int_{\Gamma} \mathbf{h}^T v \cdot n d\Gamma \quad (21)$$

where  $\mathbf{q}$  is a vector of nodal discharges, and  $\mathbf{h}^T$  is a vector of element by element defined basis functions. The constant out of plane thickness of the element is given by  $b$ , which is unity for plane flow or equal to fracture aperture for fracture flow applications. Identities (8) and (20) are fully compatible in a rigorous fashion. Interelement flow continuity is maintained

between boundary and domain formulations in a straightforward manner.

#### Boundary Conditions

Simultaneous solution of (19) is only possible if either head or velocity boundary conditions are prescribed at all nodes of the boundary solution domain. Since, in general, the boundary nodes that interface directly with the finite element mesh will have "a priori" undefined boundary conditions, it is necessary to prescribe artificial boundary conditions to aid the symbolic inversion of (20). Column substitution is first completed to move all nodal quantities corresponding to known total head and, as yet, unconstrained head boundary conditions to the right-hand side of (19). The right-hand side is completely defined if, for all the unconstrained nodes, the head at one node is held at unity and all others are set to zero. The system of equations may then be solved. When repeated for all unconstrained nodes this procedure results directly in a geometric conductance matrix linking nodal heads to nodal discharges. If  $l$  prescribed head nodes exist on a boundary domain of  $m$  nodes then the resulting geometric conductance matrix from the boundary solution procedure is fully populated and  $l \times l$  in dimension. Thus the symbolic inversion of (20) is equivalent to solving a system of  $m$  equations for  $l$  different solution vectors.

All nodes corresponding to prescribed velocity boundary conditions are effectively condensed out and no equations require to be set up in the following coupled solution of the finite element and boundary element geometric conductance matrices [Elsworth, 1986b]. Equation (20) represents the geometric conductance matrix for a single multinoded element. The conductance matrix may be directly substituted into standard finite element matrix assembly routines as a single multinoded element with appropriate nodal connections. For linear flow, the matrix entries for the boundary element domain are invariant and require to be evaluated only once.

#### Matrix Symmetry

No particular problems arise in coupling boundary and domain methods if the boundary solution matrices are asymmetric, although the procedure may be expedited if both system matrices are symmetric. If a variational formulation is adopted the geometric conductance matrix (equation (20)) may be made symmetric after formation according to the method of Zienkiewicz *et al.* [1977]. In generality, different functional variation may be chosen for normal velocities  $v \cdot n$  and heads  $\phi$  along the boundary of the domain. If heads and velocities are defined by shape functions  $\mathbf{H}^a$  and  $\mathbf{H}^b$  relative to the entire boundary of the domain then

$$\phi = \mathbf{H}^a \phi \quad (22)$$

$$v \cdot n = \mathbf{H}^b v \cdot n \quad (23)$$

Nodal fluxes  $v \cdot n$  at the boundary are related to heads by the geometric conductance relationship of (20) such that

$$v \cdot n = [\Phi^{-1} \mathbf{V}] \phi \quad (20')$$

The total potential  $\pi$  of the region may be given for the case where nodal heads only are prescribed as

$$\pi = \frac{1}{2} \int_{\Gamma} (v \cdot n)^T \phi \, d\Gamma \quad (24)$$

which on substitution of (20), (22) and (23) gives

$$\pi = \frac{1}{2} \phi^T \int_{\Gamma} [[\Phi^{-1} \mathbf{V}]^T \mathbf{H}^b \mathbf{H}^a] \phi \, d\Gamma \quad (25)$$

and may be minimized appropriately to give a revised geometric conductance matrix  $\mathbf{K}$

$$\mathbf{K} = \frac{1}{2} \int_{\Gamma} [((\Phi^{-1} \mathbf{V})^T \mathbf{H}^b \mathbf{H}^a)^T + ((\Phi^{-1} \mathbf{V}) \mathbf{H}^b \mathbf{H}^a)] \, d\Gamma \quad (26)$$

where symmetry is guaranteed. The functional variation over individual elements enforced in the current formulation is identical for head and normal velocity and therefore  $\mathbf{H}^a \equiv \mathbf{H}^b$ . To guarantee matrix symmetry in the boundary element formulation, a surrogate to (26) is invoked [Banerjee and Butterfield, 1981] such that

$$\mathbf{K} = \frac{1}{2} [\Phi^{-1} \mathbf{V}]^T + (\Phi^{-1} \mathbf{V}) \quad (27)$$

to avoid the integration enforced within (26). This approach has been found to be entirely adequate as is illustrated in the following validation exercises.

#### VALIDATION

Analytical solutions for linear and nonlinear flow within simple domains are used to examine the accuracy, versatility, and utility of the proposed coupled formulation.

#### Linear Flow

The performance of the coupled procedure is first examined for the case of a concentrically holed, circular, porous disc containing both embedded and fully penetrating finite element domains. The ability to prescribe boundary conditions on a node by node basis for both the finite element and boundary element domains provides no particular differences in meshing and execution for embedded or penetrating domains. Disc geometries are illustrated in Figure 3 for the two individual cases with inner radius  $r = a$ . The variation in hydraulic potential with radius is shown in Figure 4. Excellent agreement is maintained between analytical and numerical solutions even for relatively modest nodal coverage. The presence of perpendicular corners at the interface between boundary element and finite element domains are shown not to adversely affect results.

In the case of a semi-infinite domain, the coupled solution procedure may similarly be shown to perform satisfactorily. The solution for a pressure tunnel within a saturated porous half space is used (J. W. Bray, personal communication, 1980). In this example, the direct boundary element procedure requires that the solution domain remains finite but may be expanded to considerable dimension without computational penalty. The expanded representation of the half space domain is illustrated in Figure 5. The problem geometry comprises a single circular tunnel of radius 5 m present at a depth of 40 m below the ground surface. The piezometric surface to the domain is coincident with the ground surface and unit head is applied in the tunnel annulus. The boundary element discretization comprises 48 interior and 32 exterior nodes divided between 40 three-noded elements. For the finite element domain, 8 nine-noded Lagrangian elements are used totaling 45 nodes. Zero flux boundary conditions are applied to the

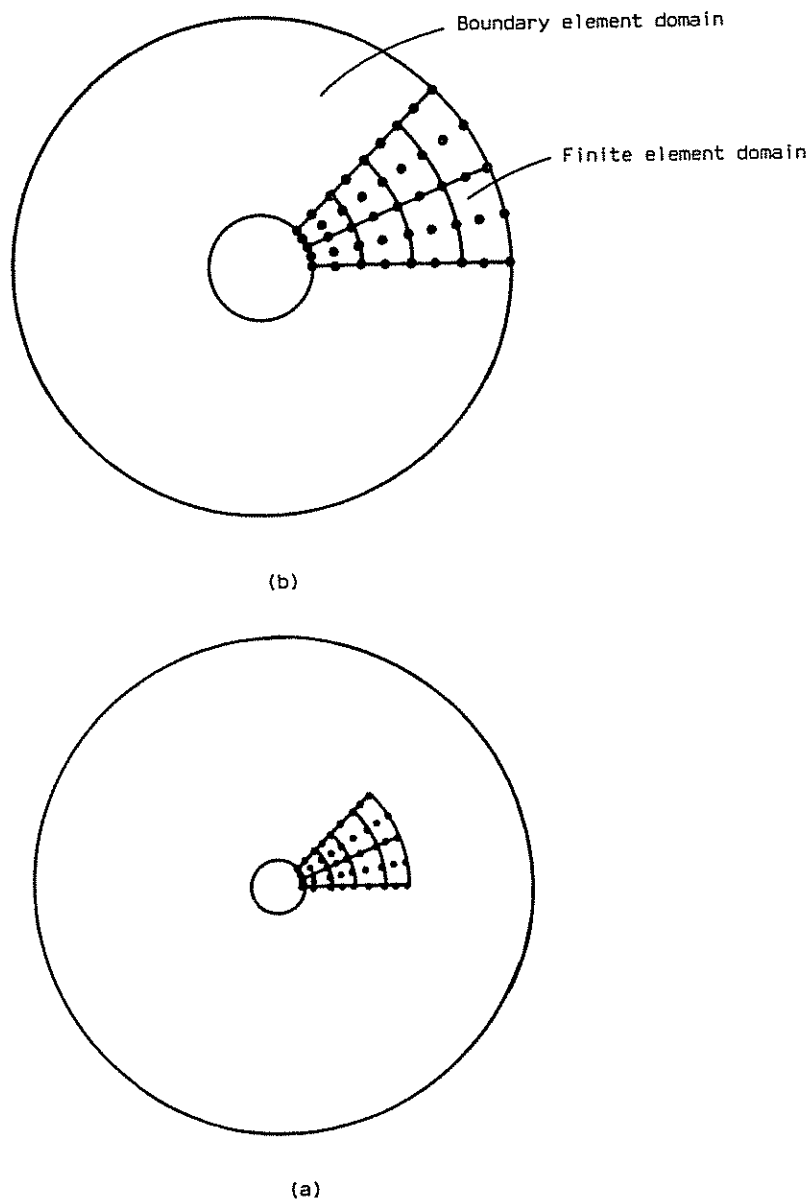


Fig. 3. Circular concentrically perforated disc with (a) embedded and (b) fully penetrating finite element domains.

lower and side elements of the boundary element exterior with the result that the conductance matrix derived from the boundary element discretization retains only 57 degrees of freedom. The assembled finite element-boundary element procedure has a total of 84 degrees of freedom. The variation in normalized hydraulic potential for the solution geometry is illustrated in Figure 6. The nodal potentials along sections A-A' and B-B' are shown to yield excellent agreement with the analytical solution. This excellent agreement is maintained despite use of relatively sparing nodal coverage in the finite element domain. Similarly, the large discrepancy in physical magnitude of the boundary element and finite element domains, as illustrated in Figure 5 has not affected solution accuracy.

In addition to being capable of representing conditions of porous media flow, the coupled model may be used in fracture flow applications. Analytical solution is available for the case of an infinite porous medium traversed by a single fracture of finite length and infinite hydraulic conductivity [Gringarten,

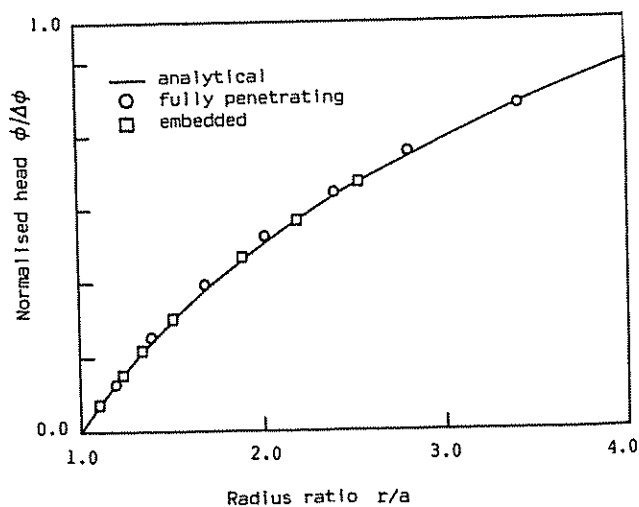


Fig. 4. Variation in normalized hydraulic head with radius for perforated disc geometries.

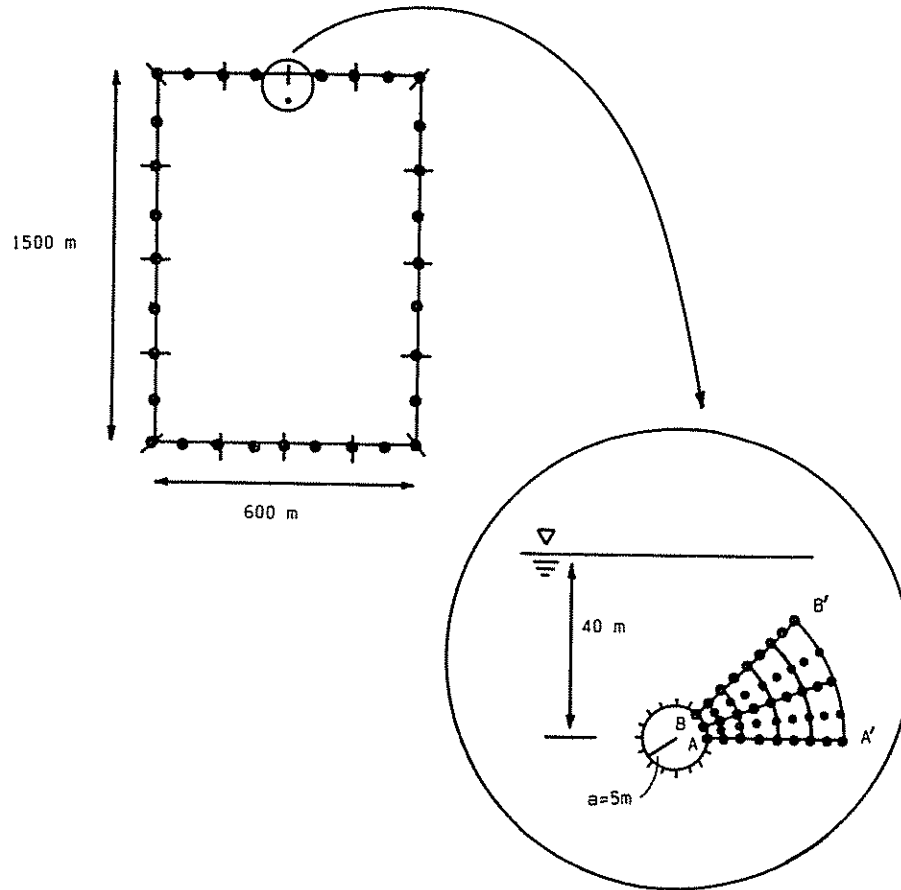


Fig. 5. Discretization geometry used for a pressure tunnel problem (to scale).

1974]. The fracture is symmetrically disposed about a central wellbore from which an infinite reservoir is pumped. The boundary element discretization of the truncated infinite domain is illustrated in Figure 7a; the internal crack is divided into 21 nodes and 10 elements, and the external boundary is divided into 16 nodes and 8 elements. The external constant potential boundary is arbitrarily located at a distance of 50 m to simulate the infinite domain. The domain external nodes are all equally spaced on the circumference although the large hydraulic gradients and velocities manifest at the crack tip are best reproduced if nodal concentrations are located at the fracture tip. The discretization density is illustrated in Figure 7a where individual elements cover 0.56, 0.24, 0.12, 0.06, and 0.02 m of the fracture half length. In accordance with a validation example reported by Shapiro and Andersson [1983], the surrounding porous medium is represented by a formation conductivity of 1 m/d and central well discharge of 1 m<sup>2</sup>/d.

The boundary element model used in this procedure uses internal slit elements to represent the internal fracture. The essential component of this element is that it allows discharge into the element from the surrounding medium on either side. The formulation of the element has been adequately described elsewhere [Elsworth, 1986a] and no further explanation will be given here. With the slit element in place within the boundary solution domain, the relevant matrix identities may be assembled and inverted to yield the geometric conductance of the system. To this condensed system, fracture line elements representing the internal fracture are added and the system solved in finite element format using a central producing wellbore. In agreement with the example completed by Shapiro

and Andersson [1983], fracture conductivities of 10<sup>4</sup> m/d are ascribed to the vertical fracture to simulate "infinite" conductivity. Using this conductivity contrast, excellent agreement between the analytical results of Gringarten [1974] and the

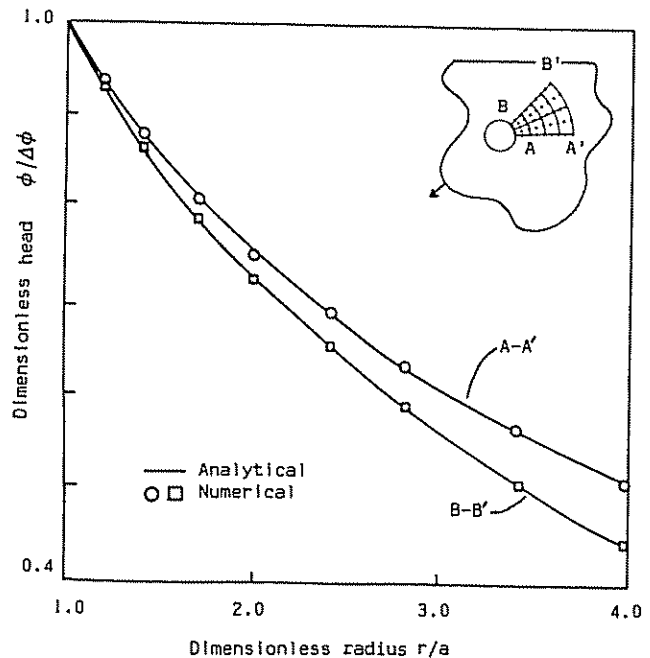


Fig. 6. Variation in total hydraulic head with radius for pressure tunnel geometry.

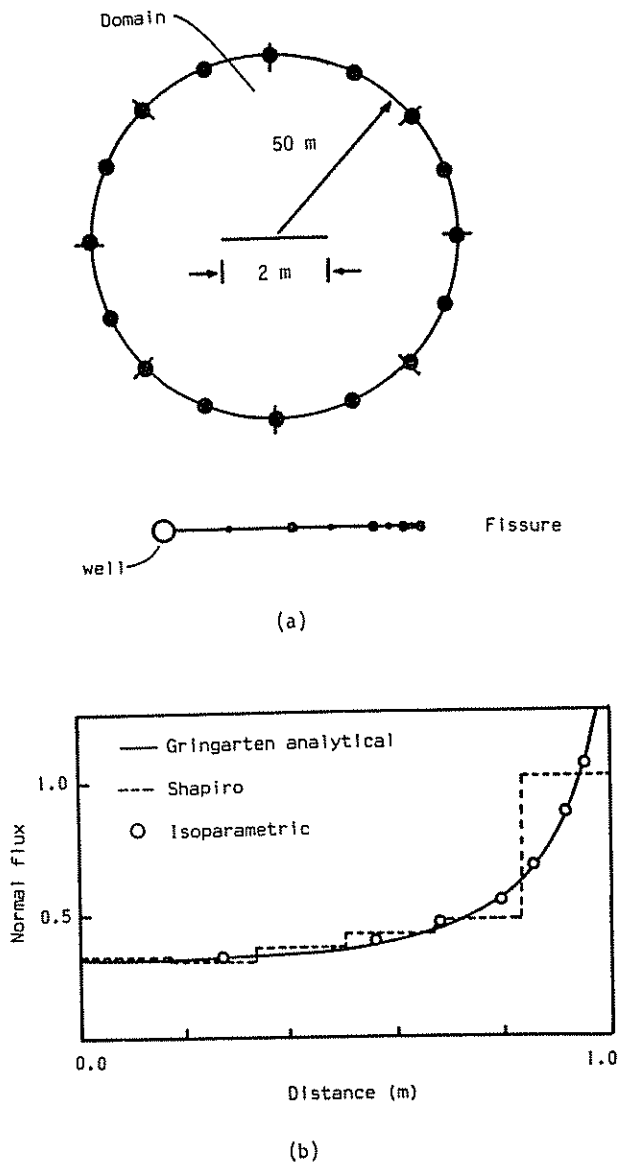


Fig. 7. Geometric representation of a fracture within a pseudo infinite porous medium (a) and results for the isoparametric model (b).

model formulated in this work are obtained. The results are illustrated in Figure 7b.

A second solution procedure may be applied to the problem whereby more note is made of the true character of the central fracture of infinite conductivity. The infinite conductivity of the fracture implies that head losses along the fracture length will be zero. Thus the only compatible solution to the problem is one in which nodal potentials along the internal slit are constant. Similarly, normal (to the fracture) mass fluxes must total  $1 \text{ m}^2/\text{d}$  when integrated over the fracture length. Therefore the problem may be solved iteratively satisfying these two internal constraints of constant potential and prescribed total normal flux. Solution by this procedure yields identical results

to those previous. Clearly, the fracture to porous medium conductivity contrast of 4 orders of magnitude used in the alternate problem treatment is sufficient to represent the infinite conductivity of the fracture. Comparison of the results from this model with those of the analytical solution illustrates the ability of the formulation to faithfully represent the high flux gradients at the crack tip. The crack tip flux is recorded at  $11.7 \text{ m/d}$  representing an asymptote set at approximately ten times the height of the figure vertical axis.

#### Nonlinear Flow

Radial flow within a single circular fracture pierced centrally by a well bore is a problem for which an analytical solution is available (B. Amadei, personal communication, 1983). For validation, an axisymmetric geometry is chosen with domain external and internal radii of 6.0 and 0.25 m respectively. Finite element discretization reaches to a radius of 2.0 m. The combined boundary element-finite element mesh illustrated in Figure 8 is used. The domain comprises 51 finite element nodes and 20 boundary element nodes. The boundary conditions for the boundary element domain are such that only six active degrees of freedom are retained in the condensed geometric conductance matrix. For a nominal fracture aperture  $b$  of 1.0 cm, fracture relative roughness  $k/2b$  of 0.5, fluid kinematic viscosity  $\nu$  of  $1.8 \times 10^{-6} \text{ m}^2/\text{s}$ , and a head differential across the system of 0.022 m, the nonlinear flow results are illustrated in Figure 9. Excellent agreement is obtained between the analytical and numerical results. The numerical results are completed using two point Gauss quadrature in evaluating the nonlinear conductance matrix integrals. For this particular example, the results following eight iteration cycles are graphically indistinguishable from those of over 20 iterations duration. Acceptable results are normally obtained after 10 iterations. It is apparent from these simple validation exercises that the proposed formulation is capable of returning satisfactory results to a variety of linear and nonlinear potential flow applications.

#### CONCLUSIONS

A coupled solution procedure is presented that is capable of representing linear and nonlinear flows in porous and fractured media. The coupling is performed in a straightforward manner through noting respective nodal conductance associations. This procedure allows arbitrarily embedded or located nonlinear zones to be easily analyzed. The boundary element domain may be simply considered as a single multinoded finite element and accommodated appropriately.

The boundary element procedure is particularly suited to representing volumetrically large or pseudo infinite domains where system matrix size or solution stability is, within reason, unaffected by domain dimension. Where prescribed flux nodes are included on the boundary element edge contour, the corresponding system equations are not retained at the global level. Depending on mesh specific details, this results in considerable computational saving both at the stage of reducing the bound-

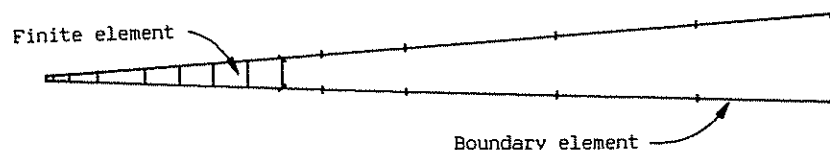


Fig. 8. Discretization of turbulent radial flow within a planar rock fracture.

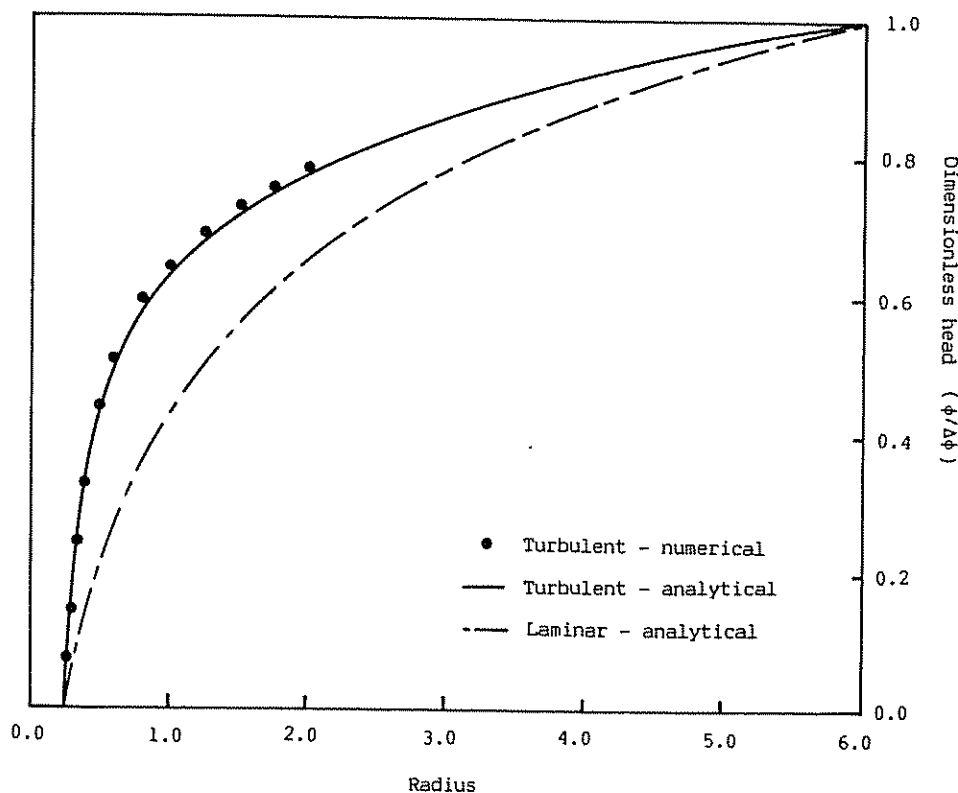


Fig. 9. Variation in normalized head with radius for turbulent radial flow within a planar rock fracture.

ary element domain and later in global system matrix assembly and solution.

The use of quadratic functional variation for both the finite element and boundary element domains ensures compatibility in the strictest sense. This facet appears especially useful in accurately representing regions of high gradient within the flow domain at crack tips and other singularities.

Nonlinear flow effects are accommodated most effectively where the nonlinearity is confined within the finite element domain. This allows the domain and integral methods to operate to maximum advantage. Since nonlinear effects, such as turbulence, are commonly of limited areal extent, coupled procedures provide a viable method of analysis. This is especially true where the zones of expected turbulence may be delimited a priori, say, by the known presence of highly conductive fractures. In other instances, where turbulent areas cannot be identified before analysis, some form of self-adaptive capability in the analysis would clearly be an advantage. Such concerns are not addressed herein. The proposed procedure is also applicable to other nonlinear flow problems.

The resulting matrix identities for the boundary element domain may be made positive definite and symmetric. This facet allows execution using readily available finite element coding arrangements accommodating storage of geometric conductance matrix terms above, and including, the leading diagonal only.

NOTATION

- $K$  hydraulic conductivity.
- $K_e$  equivalent hydraulic conductivity.
- $\bar{K}$  equivalent nonlinear hydraulic conductivity.
- $K$  geometric conductance matrix (FEM).
- $\bar{K}$  medium hydraulic conductivity tensor.
- $M$  line source or sink strength.

- $Re, Re_c$  Reynolds number, critical Reynolds number.
- $V(i, j), \Phi(i, j)$  kernel terms.
- $V, \Phi$  matrices of integrated kernel terms.
- $\mathbf{a}^T$  vector of basis function derivatives in global coordinates.
- $\bar{a}, \bar{b}$  Forchheimer equation constants.
- $b$  fracture aperture.
- $c, e$  Missbach equation constant, Missbach equation exponent.
- $c(i)$  free term.
- $g$  gravitational acceleration.
- $\mathbf{h}^T$  vector of element basis functions.
- $k$  fracture absolute roughness.
- $l$  iteration count.
- $\mathbf{n}$  domain unit outward normal.
- $q, \mathbf{q}$  discharge, vector of nodal discharges.
- $r$  radius of separation of kernel functions.
- $\mathbf{v}, v$  Darcy flow velocity, vector of nodal flow velocities.
- $x, y$  Cartesian coordinates.
- $\alpha$  turbulent flow exponent.
- $\delta_{ij}$  Kronecker delta.
- $\phi$  total hydraulic head.
- $\Omega$  domain area.
- $\Gamma$  domain external contour.
- $\xi, \eta$  local coordinates.
- $\nu$  fluid kinematic viscosity.

REFERENCES

Bachmat, Y., J. Bredehoeft, B. Andrews, D. Holtz, and S. Sebastian, *Groundwater Management: The Use of Numerical Models, Water Resour. Monogr. Ser.*, vol. 5, edited by P. van der Heijde et al., AGU, Washington, D. C., 1980.

Banerjee, P. K., and R. Butterfield, *Boundary Element Methods in Engineering Science*, McGraw-Hill, New York, 1981.

Brady, B. H. G., and A. Wassyng, A coupled boundary element-finite

- element method of stress analysis, *Int. J. Rock Mech. Min. Sci.*, 16, 235-244, 1981.
- Chen, H. S., and C. C. Mei, Oscillations and wave forces in a man-made harbor in open sea, paper presented at Proceedings, 10th Symposium on Naval Hydrodynamics, MIT, Cambridge, Mass., 1974.
- Elsworth, D., Coupled finite element/boundary element analysis for nonlinear flow in rock fractures and fracture networks, in *Proceedings of the 26th U.S. Symposium on Rock Mechanics*, pp. 633-641, Balkema Publishers, Rotterdam, 1985.
- Elsworth, D., A hybrid boundary element-finite element analysis procedure for fluid flow simulation in fractured rock masses, *Int. J. Numer. Anal. Method Geomechan.*, 10(6), 569-584, 1986a.
- Elsworth, D., A model to evaluate the transient hydraulic response of three-dimensional sparsely fractured rock masses, *Water Resour. Res.*, 22, 1809-1819, 1986b.
- Gringarten, A. C., H. J., Ramey, and R. Raghavan, Unsteady state pressure distributions created by a well with a single infinite conductivity vertical fracture, *Soc. Petr. Eng. J.*, 14, 347-360, 1974.
- Irmay, S., On the theoretical derivation of Darcy and Forchheimer formulas, *Eos. Trans. AGU*, 30, 702-707, 1958.
- Jaswon, M. A., and G. T. Symm, *Integral Equation Methods in Potential Theory and Elastostatics*, Academic, Orlando, Fla., 1977.
- Kellog, O. D., *Foundations of Potential Theory*, Dover, Mineola, N. Y., 1953.
- Leps, T. M., Flow through rockfill, in *Embankment Dam Engineering*, edited by S. G. Poulos, pp. 87-107, John Wiley, New York, 1973.
- Louis, C., A study of groundwater flow in rock and its influence on the stability of rock masses, *Rock Mech. Res. Rep.*, 10, Imperial Coll., London, September 1969.
- Neuman, S. P., Saturated-unsaturated seepage by finite elements, *J. Hydraul. Eng.*, 99(HY12), 2233-2251, 1973.
- Shapiro, A. M., and J. Andersson, Steady state fluid response of fractured rock: A boundary element solution for a coupled discrete fractured continuum model, *Water Res. Res.*, 19(4), 959-969, 1983.
- Shaw, R. P., Coupling boundary integral equation methods to other numerical techniques, in *Recent Developments in Boundary Element Methods*, Southampton University, 1978.
- Silvester, P., and M. S. Hsieh, Finite element solution of 2D exterior field problems, *Proc. Inst. Electr. Eng.*, 118(12), 1943-1947, 1971.
- Stroud, A. H., and D. Secrest, *Gaussian Quadrature Formulas*, Prentice-Hall, Englewood Cliffs, N. J., 1966.
- Volker, R. E., Nonlinear flow in porous media by finite elements, *J. Hydraul. Eng.*, 95(HY6), 2093-2114, 1969.
- Volker, R. E., Solutions for unconfined non-Darcy seepage, *J. Irrig. Drain. Div. Am. Soc. Civ. Eng.*, 101(IR1), 53-65, 1975.
- Zienkiewicz, O. C., D. W. Kelly, and P. Bettles, The coupling of the finite element method and boundary element procedures, *Int. J. Numer. Meth. Eng.*, 11, 355-375, 1977.

---

D. Elsworth, Department of Mineral Engineering, Pennsylvania State University, 104 Mineral Sciences Building, University Park, PA 16802.

(Received September 11, 1985;  
revised December 12, 1986;  
accepted December 24, 1986.)